

# DESIGN STUDY OF A MEBT WITH AN ANTI-CHOPPER FOR THE JKJ

S. Wang\*, S. Fu, IHEP, Beijing, China  
T. Kato, KEK, Tsukuba-shi, Ibaraki-ken, Japan

## Abstract

The medium-energy beam-transport line (MEBT) plays an important role in reducing beam losses in the JAERI KEK Joint project (JKJ). A MEBT was designed and constructed, with good beam matching and lower beam losses. To further reduce beam losses during the transient time of the chopper, a medium-energy beam-transport line with an anti-chopper has been designed. The 3.6m long transport line consists of 10 quadrupoles magnets, three bunchers and four chopper/anti-chopper cavities. It accomplishes three tasks: matching the beam from the RFQ to the acceptance of the DTL, chopping the beam to produce gaps for injection into the rapid-cycling ring which follows the linac, and returning the partly deflected beam back to the acceptance of the DTL. An RF chopper and an anti-chopper have been adopted in the lattice, and the choices of the parameter of chopper cavity are discussed. Details of the beam dynamics analysis are given.

## 1 INTRODUCTION

From the point of view of either the pulse current or the average current, the beam intensity in the linac of the JAERI/KEK project is high. Beam-loss control is a very essential requirement in accelerator design and performance to avoid strong radioactivity induced by lost particles. In the linac design of the JAERI/KEK project, the Medium-Energy Beam-Transport line (MEBT), between RFQ and DTL, plays an important role in beam-loss control. It accomplishes beam matching and chopping. These two tasks have a close relation with beam-loss control. Beam matching is very important to minimize the growth of emittance and avoid beam-halo formation, which has been recognized as one of the major causes for beam loss[1]. Clean chopping is also a key point for beam-loss control. In the JAERI/KEK project, 500  $\mu$ sec long macropulses from the ion source needs to be chopped into sub-pulses for injecting into the following 3 GeV rapid-cycling ring. The sub-pulse consists of a 278 nsec long pulse and a 222 nsec gap. The chopped pulse should have a clean cut at the head and the tail of the pulse so as to avoid beam losses at later parts of the linac or during injection into the ring.

A MEBT for JHF was designed and constructed, with good beam matching and lower beam losses. To further reduce the number of these unstable particles in MEBT.

The adoption of an anti-chopper is a good choice for decreasing the number of the unstable particles. Theoretically, using an anti-chopper can cancel all of the unstable particles produced during the transient time.

Based on the previous design of the MEBT, a MEBT with an anti-chopper was designed. It accomplishes matching and chopping, and cancels any unstable particles. To maintain the beam quality, increase of the length of the transport line is not too much, in spite of adding of an anti-chopper. This is a benefit from the asymmetric design. The details of the design are described in this report.

## 2 DESIGN OF THE BEAM LINE

### 2.1 The Adoption of the Asymmetric Scheme

For returning partly deflected beams back to the beam axis by using an anti-chopper, the symmetric design is a direct idea of using an anti-chopper, just like in the case of the SNS MEBT[2]. When using a symmetric design, the arrangement of elements between the chopper and anti-chopper is symmetric. However, some extra elements are needed just to maintain the symmetry. The key problem is that the symmetric arrangement makes the envelope at the location of the anti-chopper hard to control, and the aperture of the anti-chopper is a bottle neck of the MEBT. The adoption of the asymmetric scheme is a good choice. The feasibility of asymmetric scheme has been proved[3].

### 2.2 Design of the MEBT with an anti-chopper

A modified TRACE3D[4] is used to describe the deflection behavior of the chopper and the anti-chopper. It includes the element of an RF deflector. The field distribution of the deflector was obtained from MAFIA results, including the fringe fields beside the deflecting electrode. The beam parameters at the entrance of the MEBT (exit of RFQ) are listed in the table 1.

Table 1 Beam parameters at the MEBT entrance

| I(mA) | $\epsilon^{x,y}_{RMS}(\pi\text{mm-mrad})$ | $\epsilon^z_{RMS}(\pi\text{MeV-degree})$ |
|-------|---|--|
| 50    | 0.200                                     | 0.150                                    |

\*E-mail: wangs@ihep.ac.cn

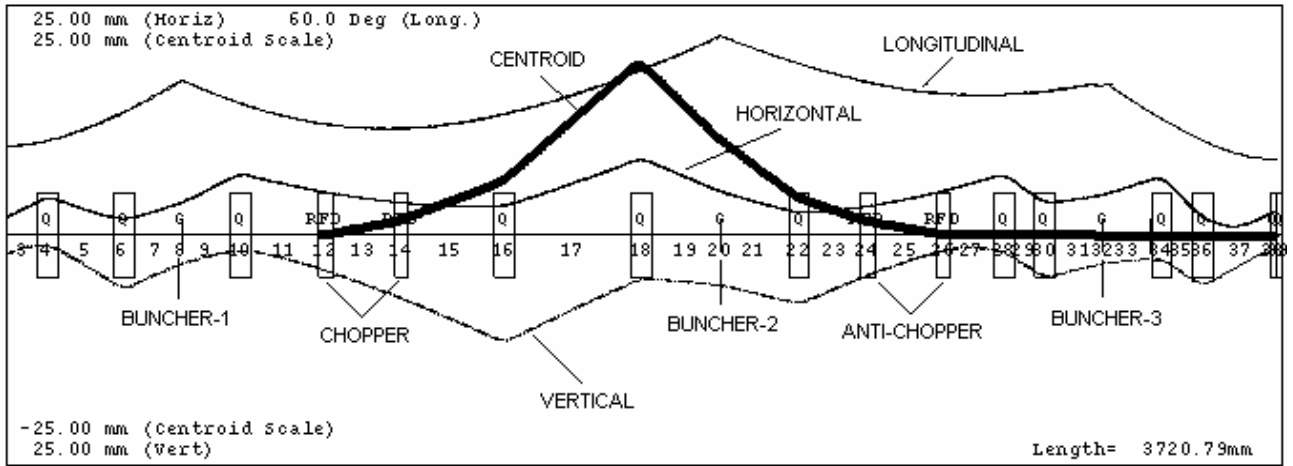


Figure 1. TRACE 3-D output of MEBT with an anti-chopper. The beam profiles in the z, x and y directions are shown respectively. The coarse line traces the beam centroid deflected by two RF choppers and two RF anti-choppers.

The first half of the beam line, upstream of element 18, is mainly aimed at obtaining a large separation between the chopped beam and the unchopped beam at element 18. In this part, the arrangement of elements remains the same as that of the previous MEBT design, and uses the same RF deflectors as a chopper. Regardless the head and the tail of a bunch, the edge separation between a full-chopped beam and an unchopped beam is 4 mm at the scraper, when both RF deflectors have a deflecting field of 1.9MV/m (corresponding to 27KW power input). For deflecting the head and the tail of the bunch, much more power input is needed.

The second part of the beam line, downstream of element 18, should accomplish two tasks: returning a partly deflected beam back to the beam axis and matching the unchopped beam with the acceptance of the DTL.

A similar type RF deflector as the chopper is adopted as an anti-chopper. Taking the advantage of asymmetric scheme, the deflecting field can be different from that of chopper. In the design of figure 1, a deflecting field of 1.7 MV/m is adopted in the anti-chopper. When the power input of the chopper deflector is changed, tuning the beam-line parameter of element 18th to 25th can satisfy the requirement of anti-chopper, without changing the power input of the anti-chopper deflector. Thus, the power input of the anti-chopper deflector can be fixed. The other four quadrupoles, downstream of the anti-chopper, are used to match the transverse phase space to the acceptance of the DTL.

There are three bunchers in the beam line to keep the bunch length from increasing too much. Two bunchers are needed for matching the longitudinal phase space to the acceptance of the DTL. Three bunchers make it easy to control the bunch length at the deflector, and also make it possible to make the bunch length close to each other at the chopper deflectors and the anti-chopper deflectors.

### 2.3 Elements Used in the Beam Line

Table 2 gives the total number of elements used in the beam line with the anti-chopper, compared with the

previous no anti-chopper beam line. Except for the deflector, all of the elements are the same as those used in the no anti-chopper beam line.

In the previous design, to decrease the number of the partly deflected bunches, the deflector reach a very fast rise time. Because of adopting an anti-chopper, it is possible to allow proper longer rise time by changing the coupling of deflector cavity, to obtain higher deflection field.

Table 2. Elements number used in the beam line

| Anti-chopper | Q  | deflector | Buncher | Length(m) |
|--------------|----|-----------|---------|-----------|
| Yes          | 10 | 4         | 3       | 3.6       |
| No           | 8  | 2         | 2       | 2.9       |

## 3 THE OPTIMIZATION OF ANTI-CHOPPER

A similar type rf deflector is adopted as an anti-chopper. The gap between two electrodes of the anti-chopper deflector increased to 12mm, while that of chopper deflector is 10mm. The larger gap is required to ensure no particle is lost on the electrode. To get the same deflecting voltage, the larger gap means larger input power requirement. The maximum capability of the up-to-date solid power supply is 30KW. To decrease the demand of the input power, some further optimization are proposed.

To minimize the demand power  $P$ , a large value of  $Z/Q_0$  should be pursued according to an approximate relation

$$P \cong \frac{V^2}{\omega_0 \tau (Z/Q_0)}$$

in which  $V$  is the deflecting voltage,  $\omega_0$  the frequency,  $\tau$  the rise time,  $Z$  the transverse shunt impedance and  $Q_0$  the unloaded  $Q$  value. To get the higher value of  $Z/Q_0$ , the cuboid electrode is replaced by a stem plus electrode structure, as showed in the figure 2. The size of the top surface of the electrode is kept unchanged.

Table 3 show the compare of the  $Z/Q_0$  between cuboid electrode structure and stem structure. The value of  $Z/Q_0$  is increased by a factor of 17%.

To reach fast rise time, two large coupling loops are used in rf deflector. In chopper deflector, two large loops are placed asymmetrically with respect to the middle plane to get larger bandwidth. This induces an asymmetric spectrum with respect to central frequency, and the high frequency side is wider than the other side[5]. For chopper deflector, the high frequency side is 18MHz, and the low frequency side is 12MHz, while in case of symmetric placement of loops, the low frequency side and the high frequency side are all 12 MHz. The simulation by using T3 module of MAFIA shows that for an rf deflector, the symmetric and asymmetric arrangement of the coupling loops do not effect the rise time, while the symmetric placement has a symmetric spectrum and a wider mode separation. The further experimental study is necessary to determine the placement of the coupling loops.

Table 3 The  $Z/Q_0$  with different electrode structure

| Type   | $Q_0$   | Z      | $Z/Q_0$ |
|--------|---------|--------|---------|
| Cuboid | 1.102e4 | 4.87e6 | 442     |
| Stem   | 1.034e4 | 5.35e6 | 517     |

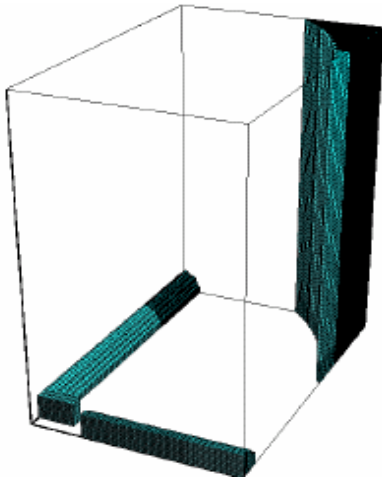


Figure 2 The structure of the new electrode of rf deflector

#### 4 BEAM DYNAMICS SIMULATION

The beam dynamics of the beam line was studied using PARMILA. Figure 3 shows the simulation results of the emittance growth along the MEBT. Although an anti-chopper was added and the total length was increased to 3.5m, the RMS emittance growth is still less than 16%. No extra emittance growth exists compared with that of the previous no anti-chopper design.

Figure 4 shows the phase space of a 60% deflected beam at the entrance of the DTL. The partly deflected beam is returned back to the beam axis by the anti-chopper, within the acceptance of the DTL.

#### 5 CONCLUSION

Based on the previous MEBT design, a MEBT with an anti-chopper has been designed for matching and cleanly chopping beam. Taking the advantage of the asymmetric

scheme, the design is much more flexible and can use different deflectors for the chopper and the anti-chopper. To decrease the demanded power of anti-chopper deflector, some further optimisation for rf deflector are proposed. Simulation results show that there is no extra emittance growth due to the use of an anti-chopper, and that all of partly chopped beam can be returned back to the acceptance of the DTL.

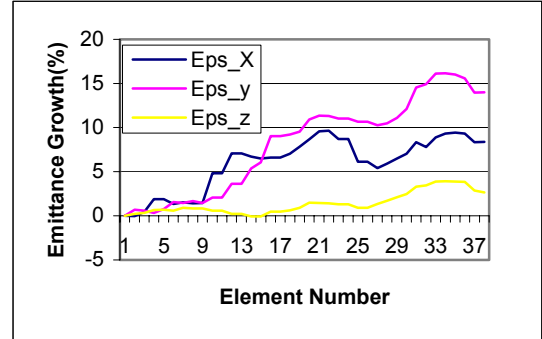


Figure 3. RMS Emittance growth along the beam line.

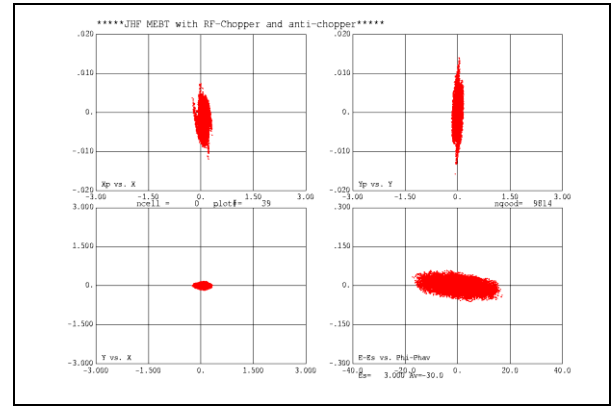


Figure 4. Phase space of a beam deflected by the chopper and the anti-chopper at entrance of the DTL.

#### REFERENCES

- [1] Y.Yamazaki, "Design Issues for High-Intensity, High Energy Proton Accelerators", Proc. of 1996 Inter. Linac Conf. Geneva, p26, August 1996.
- [2] J.Staples, D.Oshatz, et al. "Design of the SNS MEBT", LINAC'2000, Monterey, MOD18, August, 2000
- [3] S.Wang S. Fu and T.Kato, Design of a Medium-Energy Beam Transport Line With an Anti-Chopper for the JAERI/KEK Project, Proceedings of the 26<sup>th</sup> Linear Accelerator Meeting in Japan, p79, Aug. 2001 Tsukuba, Japan
- [4] T.Kato, S.Fu, "MEBT Design for the JHF 200-MeV Proton Linac", LINAC'98, Chicago, p70, August 1998.
- [5] S.Fu, T.Kato, "RF-Chopper for JHF Linac", Nucl. Instr. & Meth. in Phy. Res., Section A. p296, Vol.440. 2000.